DOI: 10.1002/cmdc.201300479

Anticancer Potential of (Pentamethylcyclopentadienyl)chloridoiridium(III) Complexes Bearing κ*P* and κ*P*,κ*S*-Coordinated $Ph_2PCH_2CH_2CH_2S(O)_xPh$ ($x = 0–2$) Ligands

Gerd Ludwig,[a] Ivan Ranđelović,[b] Danijela Maksimović-Ivanić,[b] Sanja Mijatović,[b] Mirna Z. Bulatović,[b] Djordje Miljković,[b] Marcus Korb,[c] Heinrich Lang,[c] Dirk Steinborn,[a] and Goran N. Kaluđerović*[a]

Iridium(III) complexes of the type $[Ir(\eta^5\text{-}C_5Me_5)Cl_2\{Ph_2PCH_2CH_2CH_2S(O)_xPh\text{-}\kappa P\}]$ ($x = 0–2$; **1**–**3**) and $[Ir(\eta^5\text{-}C_5Me_5)Cl\{Ph_2PCH_2CH_2CH_2S(O)_xPh\text{-}\kappa P,\kappa S\}][PF_6]$ ($x = 0–1$; **4** and **5**) with 3-(diphenylphosphino)propyl phenyl sulfide, sulfoxide, and sulfone ligands $Ph_2PCH_2CH_2CH_2S(O)_xPh$ were designed, synthesized, and characterized fully, including X-ray diffraction analyses for complexes **3** and **4**. In vitro studies against human thyroid carcinoma (8505C), submandibular carcinoma (A253), breast adenocarcinoma (MCF-7), colon adenocarcinoma (SW480), and melanoma (518A2) cell lines provided evidence for the high biological potential of the neutral and cationic iridium(III) complexes. Neutral iridium(III) complex **5** proved to be the most active, with IC_{50} values up to about 0.1 μM, representing activities of up to one order of magnitude higher than cisplatin. Using 8505C cells, apoptosis was shown to be the main mechanism through which complex **5** exerts its tumoricidal action. The described iridium(III) complexes represent potential leads in the search for novel metal-based anticancer agents.

Introduction

Bioinorganic chemistry is a fascinating and creative area full of possibilities.[1] One of the earliest examples, which clarifies this statement, was the discovery of the biological potential of cisplatin by Rosenberg in 1965.[2,3] Cisplatin itself can still be considered the "gold standard" for all metal-based anticancer drugs that followed.[4] Despite the success of cisplatin and other platinum-based anticancer drugs, further transition-metal complexes were examined for their cytotoxic activity. This can be explained, among other things, by the drawbacks of cisplatin, such as dose-dependent side effects and the partial resistance of some carcinomas.[5–10] Thus, other metal-based anticancer agents (M = Ti, Ru, Au, …) were tested for their biological potential, and compounds like the octahedral ruthenium complexes [imiH]*trans*-[Ru(imi-κ*N*)(DMSO-κ*S*)Cl_4] (imi = imidazole; DMSO = dimethylsulfoxide) and [indH]*trans*-[Ru(ind-κ*N*)$_2Cl_4$] (ind = indazole) demonstrated their potential and entered clinical trials.[11–17] The analogous iridium complexes, [imiH]*trans*-[Ir(imi-κ*N*)(DMSO-κ*S*)Cl_4] and [indH]*trans*-[Ir(ind-κ*N*)$_2Cl_4$],[18] and other iridium(III) complexes proved to be less active or inactive[19–26] due to the kinetic inertness of low-spin d^6 Ir^{III} complexes.[27] Nevertheless, iridium-based anticancer agents, such as the *fac*-[Ir(N^N)(DMSO-κ*S*)Cl_3] (N^N = diimine-type ligand as in **I**), with high biological potential have been prepared.[28] Further steps were taken in the field of iridium-based anticancer agents with the preparation of η^5-pentamethylcyclopentadienyl iridium(III) complexes of the type $[Ir(\eta^5\text{-}C_5Me_5)Cl(X^Y)]^{n+}$ (X^Y = bidentate ligand), but these complexes with *N*,*N*′ ligands (X^Y = ethylendiamine, 2,2′-bipyridine, 1,10-phenanthroline)[29] and $[Ir(\eta^5\text{-}C_5Me_5)Cl_2(PTA)]$ (PTA = 1,3,5-triaza-7-phosphaadamantane)[24] showed no activity when evaluated in vitro cytotoxic studies. As presented by Sheldrick et al.[30] and Sadler et al.,[29] the incorporation of a functionalized bipyridine/phenanthroline or C_5Me_5 ligand in the above-mentioned types of compounds resulted in highly active iridium(III) complexes (e.g., complexes **II** and **III**). Another way to increase the cytotoxic activity of these complexes is to exchange the neutral diimine-type ligand for an anionic N^C ligand (complex **IV**). For this type of complex, IC_{50} values in the range exhibited by cisplatin were observed.[31,32]

Previously, our group made some promising steps in the field of iridium-based anticancer compounds by showing the biological potential of neutral and cationic iridium(III) complexes with (diphenylphosphino)methyl phenyl sulfide, sulfoxide and sulfone ligands (**V** and **VI**).[33] Here, we report the design, synthesis and biological potential of neutral and cationic iridium(III) complexes with 3-(diphenylphosphino)propyl

[a] G. Ludwig, Prof. Dr. D. Steinborn, Prof. Dr. G. N. Kaluđerović
Institute of Chemistry, Martin Luther University Halle-Wittenberg
Kurt-Mothes-Straße 2, 06120 Halle (Germany)
E-mail: goran.kaluderovic@chemie.uni-halle.de

[b] I. Ranđelović, Dr. D. Maksimović-Ivanić, Dr. S. Mijatović, M. Z. Bulatović, Dr. D. Miljković
Institute for Biological Research "Sinisa Stankovic", University of Belgrade
Bulevar despota Stefana 142, 11060 Belgrade (Serbia)

[c] Prof. M. Korb, Prof. Dr. H. Lang
Institute of Chemistry, Chemnitz University of Technology
Straße der Nationen 62, 09111 Chemnitz (Germany)

Supporting information for this article is available on the WWW under http://dx.doi.org/10.1002/cmdc.201300479.

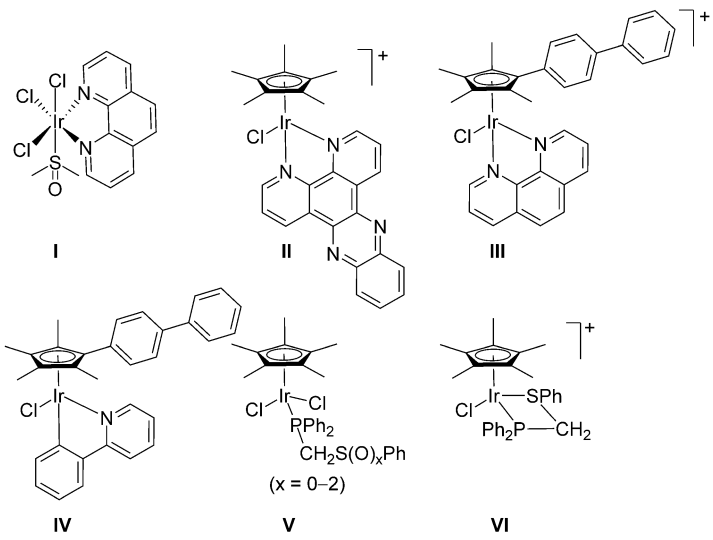

phenyl sulfide, sulfoxide and sulfone ligands of the type $[Ir(\eta^5\text{-}C_5Me_5)Cl_2\{Ph_2PCH_2CH_2CH_2S(O)_xPh\text{-}\kappa P\}]$ (x = 0–2; complexes **1**–**3**) and $[Ir(\eta^5\text{-}C_5Me_5)Cl\{Ph_2PCH_2CH_2CH_2S(O)_xPh\text{-}\kappa P,\kappa S\}][PF_6]$ (x = 0–1; complexes **4** and **5**). Furthermore, structure–activity relationships surrounding the spacer length ($CH_2CH_2CH_2$ vs CH_2) and the oxidation state of the sulfur atom (SPh vs S(O)Ph vs $S(O)_2Ph$) are discussed.

The complexes were characterized by elemental analyses, ^1H, ^{13}C, and ^{31}P NMR spectroscopy, and single-crystal X-ray structure analyses (for **3** and **4**). Selected NMR spectroscopic data for complexes **1**–**5** are given in Table 1. For the neutral iridium(III) complexes, coordination-induced shifts (CIS) of the phosphorus resonances ($\delta_{P(coord.)}-\delta_{P(uncoord.)}$) between $\delta = 13$ and 14 ppm were observed. In contrast, the CIS of the cationic iridium(III) complexes **4** and **5** ($\kappa P,\kappa S$-coordination) were found to be much smaller (ca. $\delta = 2$ ppm). ^1H and ^{13}C chemical shifts of the ligands are largely independent from the type of the coordination (κP vs κP, κS), and the resonances of the $\eta^5\text{-}C_5Me_5$ ligand also proved to be virtually independent of the type of $S(O)_x$ functionalization.

Crystals of $[Ir(\eta^5\text{-}C_5Me_5)Cl_2\{Ph_2PCH_2CH_2CH_2S(O)_2Ph\text{-}\kappa P\}]$ (**3**) and $[Ir(\eta^5\text{-}C_5Me_5)Cl\{Ph_2PCH_2CH_2CH_2SPh\text{-}\kappa P,\kappa S\}][PF_6]$ (**4**) suitable for X-ray diffraction analyses were obtained from solutions of dichloromethane/*n*-pentane at room temperature. Neutral iridium(III) complex **3** crystallized as an isolated molecule without unusual intermolecular interactions (shortest distance between non-hydrogen atoms: O1···C4′ 2.975(9) Å). Cationic iridium(III) complex **4** crystallized in discrete cations and anions (shortest distance between non-hydrogen atoms: C2···F2 2.982(4) Å). The structures of the two complexes are presented in Figure 1, and selected structural parameters are given in the figure caption.

Table 1. Selected NMR spectroscopic data of $[Ir(\eta^5\text{-}C_5Me_5)Cl_2\{Ph_2PCH_2CH_2CH_2S(O)_xPh\text{-}\kappa P\}]$ (**1**–**3**) and $[Ir(\eta^5\text{-}C_5Me_5)Cl\{Ph_2PCH_2CH_2CH_2S(O)_xPh\text{-}\kappa P,\kappa S\}][PF_6]$ (**4** and **5**).

Compd	$Ph_2PC_\gamma H_2C_\beta H_2C_\alpha H_2S(O)_xPh$[a]						C_5Me_5[a]	
	x[b]	$\delta_{\alpha\text{-}C}$	$\delta_{\beta\text{-}C}$	$\delta_{\gamma\text{-}C}$ ($^1J_{P,C}$)	δ_P	δ_H ($^4J_{P,H}$)	δ_{CMe} ($^3J_{P,C}$)	δ_C ($^2J_{P,C}$)
1	0 (κP)	37.2	21.9	25.1 (36.2)	−2.4	1.26 (2.4)	8.2 (0.7)	97.3 (2.1)
2	1 (κP)	58.0	17.6	26.9 (33.6)	−3.0	1.33 (2.2)	8.1 (1.0)	92.1 (2.9)
3	2 (κP)	37.2	24.2	56.2 (35.5)	−2.4	1.21 (2.2)	8.7 (0.7)	96.3 (2.6)
4	0 ($\kappa P,\kappa S$)	37.5	22.3	25.7 (36.4)	−14.5	1.22 (2.4)	8.3 (0.7)	97.8 (2.1)
5	1 ($\kappa P,\kappa S$)	55.5	17.2	25.1 (37.4)	−14.1	1.26 (2.4)	8.0	100.7 (1.5)

[a] δ values are given in ppm; the corresponding J value in Hz is given in parentheses. [b] The coordination mode of the ligand is given in parentheses.

Results and Discussion

Syntheses and characterization

Neutral iridium(III) complexes of the type $[Ir(\eta^5\text{-}C_5Me_5)Cl_2\{Ph_2PCH_2CH_2CH_2S(O)_xPh\text{-}\kappa P\}]$ (**1**–**3**) bearing κP-coordinated ligands with pendant sulfide, sulfoxide and sulfone groups were synthesized according to Scheme 1 a. Under cleavage of the Ir–Cl–Ir bridges of the starting dinuclear iridium complex, formation of the mononuclear complexes **1**–**3** could be afforded in yields between 63 and 74%. The desired cationic complexes of the type $[Ir(\eta^5\text{-}C_5Me_5)Cl\{Ph_2PCH_2CH_2CH_2S(O)_xPh\text{-}\kappa P,\kappa S\}][PF_6]$ (**4** and **5**) were accessed through the subsequent reaction of neutral iridium(III) complexes **1** and **2** with $[NH_4][PF_6]$ (Scheme 1 b) in yields of 63% (**4**) and 70% (**5**). All complexes were found to be stable in air over a period of weeks and soluble in DMSO and in dichloromethane.

The main structural feature is that both complexes adopt a half-sandwich ("piano stool") conformation. In the case of neutral complex **3**, the coordination sphere of iridium(III) is built up by an $\eta^5\text{-}C_5Me_5$ ligand (distance Ir···ring centroid: 1.823 Å), two chlorido ligands, as well as the $Ph_2PCH_2CH_2CH_2S(O)_2Ph\text{-}\kappa P$ ligand. The coordination sphere of iridium(III) in complex **4** is completed by an $\eta^5\text{-}C_5Me_5$ ligand (distance Ir···ring centroid: centroid 1.849 Å), a chlorido ligand, as well as the chelating ligand $Ph_2PCH_2CH_2CH_2SPh\text{-}\kappa P,\kappa S$. In complex **3**, the angles at the iridium(III) atom are close to 90° (87.8(7)–90.4(7)°), so the structure can be considered a distorted octahedron. Due to the $\kappa P,\kappa S$ coordination of the ligand (S1–Ir–P1 87.4(3)°) in **4**, the devia-

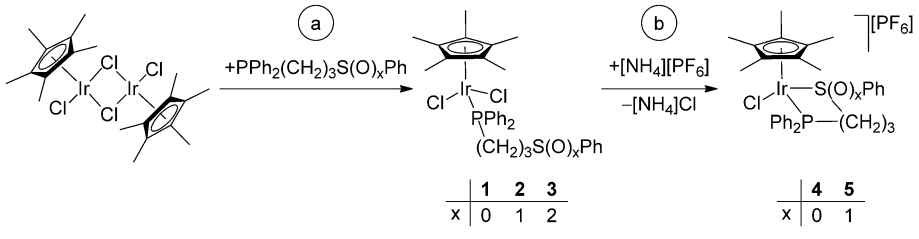

Scheme 1. Synthetic routes to iridium(III) complexes bearing $Ph_2PCH_2CH_2CH_2S(O)_xPh\text{-}\kappa P$ (**1**–**3**) and $Ph_2PCH_2CH_2CH_2S(O)_xPh\text{-}\kappa P$, κS (**4** and **5**) ligands.

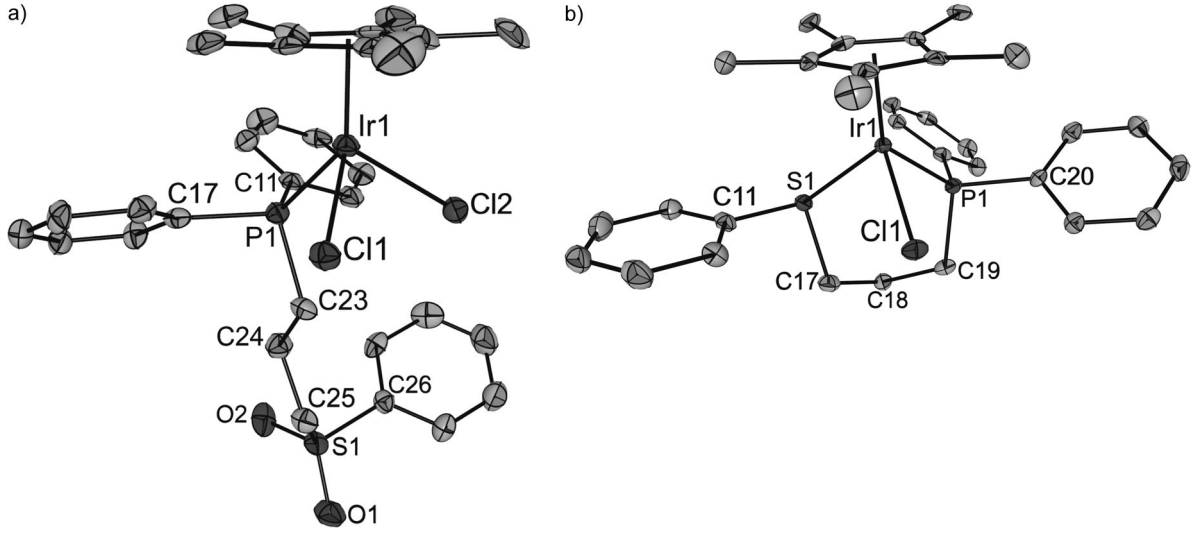

Figure 1. Single-crystal X-ray diffraction structures of a) $[Ir(\eta^5\text{-}C_5Me_5)Cl\{Ph_2PCH_2CH_2CH_2S(O)_2Ph\text{-}\kappa P\}]$ in crystals of **3** and b) $[Ir(\eta^5\text{-}C_5Me_5)Cl\{Ph_2PCH_2CH_2CH_2SPh\text{-}\kappa P,\kappa S\}]^+$ in crystals of **4**. The ellipsoids are shown with a probability of 50%. H atoms have been omitted for clarity. Selected structural parameters (distances in Å, angles in °): Ir1–Cl1 2.424(2), Ir1–Cl2 2.418(2), Ir1–P1 2.302(2), Cl1–Ir1–Cl2 90.4(7), Cl1–Ir–P1 88.0(7), Cl2–Ir–P1 87.8(7), C25–S1–C26 105.2(4), O1–S1–O2 118.5(4) for complex **3**; Ir1–Cl1 2.402(9), Ir1–S1 2.357(9), Ir1–P1 2.310(1), Cl1–Ir1–S1 93.2(3), Cl1–Ir–P1 86.5(3), S1–Ir–P1 87.4(3), C11–S1–C17 97.92(17), C11–S1–Ir1 112.58(1), C17–S1–Ir1 97.9(2) for complex **4**.

tions of 90° are slightly higher (86.5(3)–93.2(3)°). The six-membered $IrPC_3S$ iridacycle in **4** possesses a chair conformation, with atoms Ir1 and C17 forming the apices. Bond lengths of Ir–Cl (2.402(9)–2.424(3) Å) and Ir–P (2.302(3)/2.310(1) Å) in both complexes, and additionally Ir–S (2.357(9) Å in complex **4**, are in the expected range (median Ir–Cl: 2.419 Å, lower/upper quartile: 2.315/2.606 Å, $n=543$; median Ir–P: 2.316 Å, lower/upper quartile: 2.151/2.462 Å, $n=543$; median Ir–S: 2.357 Å, lower/upper quartile: 2.244/2.423 Å, $n=148$).[34]

Biological studies

To determine the biological potential of iridium(III) complexes **1**–**5**, in vitro cytotoxicity studies were performed against human thyroid carcinoma (8505C), submandibular carcinoma (A253), breast adenocarcinoma (MCF-7), colon adenocarcinoma (SW480), and melanoma (518A2) cell lines. The cells were cultured in the presence of various concentrations of the corresponding iridium complexes, and the cell viability was analyzed using sulforhodamine B (SRB) microculture colorimetric assay.[35] According to the obtained results, all complexes cause a dose-dependent decrease in cell viability (Figure 2). The IC_{50} values of iridium(III) complexes **1**–**5** are listed in Table 2; the activities of cisplatin are included for comparison. For further understanding, the IC_{50} values of the corresponding ligands **L1**–**L3** and related ruthenium(II) complexes are given in Table S1 in the Supporting Information.[36,37] Furthermore, IC_{50} values of analogous iridium(III) complexes bearing a methylene spacer (Ph_2PCH_2-$S(O)_xPh$), instead of $Ph_2PCH_2CH_2CH_2S(O)_xPh$ ligands **L1**–**L3**, are presented in Table S2 in the Supporting Information.[33]

Without exception, non-coordinated phosphino-sulfide **L1**, phosphino-sulfoxide **L2** and phosphino-sulfone **L3** ligands possess 10- to 400-times lower activities in vitro than the related iridium(III) complexes **1**–**5** (cf. data in Table 1 vs Table S1 in the Supporting Information).[36] Except for complex **3**, both the neutral and cationic iridium complexes exhibited an up to 25-times higher antiproliferative activity than cisplatin; even against cisplatin-resistant cell lines 8505C, MCF-7 and SW480 high activities were found. In the examined series, the iridium(III) complex with the highest activity proved to be complex **5** against the MCF-7 cell line, with an IC_{50} value of 0.1 μM (c.f., cisplatin: $IC_{50}=2.0$ μM). For the neutral iridium complexes, a direct correlation between the oxidation state of the pendant $S(O)_xPh$ ($x=0$–2) group of the ligand and the cytotoxic activity could be determined. Namely, the in vitro activity increases in the following order: $S(O)_2 < S(O) < S$. This trend is particularly apparent when comparing the IC_{50} values of iridium(III) complexes **1**–**3** against the 8505C cell line. Thus, neutral iridium(III) complex **1** ($n/x=3/0$) with a κ*P* coordinated ligand and a sulfide group is 30-times more active than complex **3** ($n/x=3/2$), with a pendant sulfonyl group.

Table 2. Cytotoxicity of iridium(III) complexes **1**–**5** in comparison with cisplatin against a panel of cancer cell lines.[a]

Compd	x[b]	IC_{50} [μM][c]				
		518A2	8505C	A253	MCF-7	SW480
1	0 (κ*P*)	0.3 ± 0.1	0.2 ± 0.0	0.2 ± 0.0	0.2 ± 0.1	0.6 ± 0.2
2	1 (κ*P*)	0.7 ± 0.4	0.6 ± 0.0	0.5 ± 0.1	0.3 ± 0.0	1.0 ± 0.4
3	2 (κ*P*)	4.4 ± 2.5	5.8 ± 1.3	4.9 ± 0.1	6.7 ± 1.4	4.5 ± 0.1
4	0 (κ*P*, κ*S*)	1.0 ± 0.6	0.5 ± 0.2	0.4 ± 0.0	0.4 ± 0.1	1.0 ± 0.3
5	1 (κ*P*, κ*S*)	0.4 ± 0.2	0.3 ± 0.1	0.3 ± 0.1	0.1 ± 0.1	0.9 ± 0.4
Cisplatin		1.5 ± 0.2	5.0 ± 0.2	0.8 ± 0.1	2.0 ± 0.1	3.2 ± 0.2

[a] Human thyroid carcinoma 8505C, submandibular gland carcinoma A253, breast adenocarcinoma MCF7, melanoma 518A2 and colon cancer SW480. [b] The coordination mode of the ligand is given in parentheses. [c] The compound concentration required to inhibit 50% cell growth (IC_{50}). Data represent the mean ± standard deviation (SD) of three independent experiments performed in triplicate.

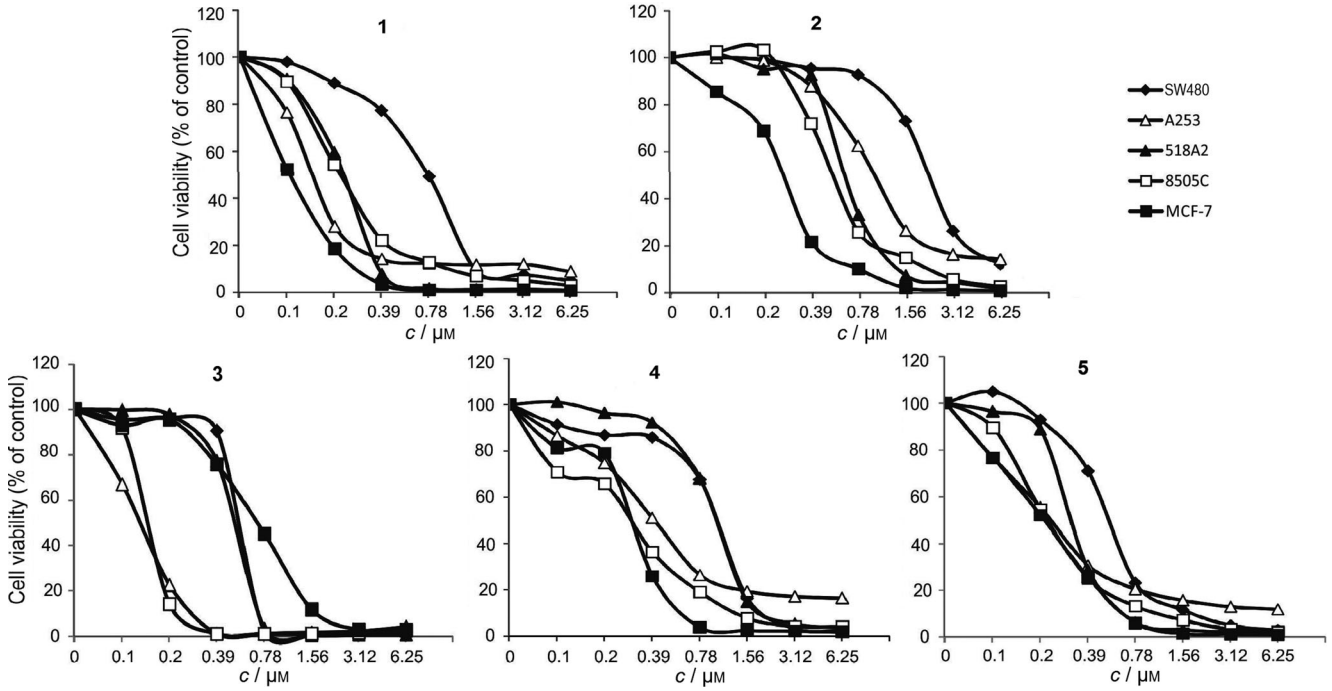

Figure 2. Representative graphs showing survival (%) of cells grown for 96 h in the presence of increasing concentrations of compounds **1**–**5**.

A direct relationship was also observed between the length of the alkanediyl spacer and cytotoxic activity. Thus, for both the neutral and the cationic iridium(III) complexes, the complexes with a trimethylene spacer possess an up to nearly two orders of magnitude higher activity than the complexes with a methylene spacer (cf. Table 1 vs Table S2 in the Supporting Information).[33] Neutral iridium(III) complexes **1**–**3** exhibited higher activities (up to two orders of magnitude) against all tested cell lines than the related ruthenium(II) complexes, $[Ru(\eta^6\text{-}p\text{-cym})Cl_2\{Ph_2PCH_2CH_2CH_2S(O)_xPh\text{-}\kappa P\}]$ ($x=0$, 1, 2) (cf. Table 1 vs Table S1 in the Supporting Information).[36] In contrast, the same tendency was not observed for cationic iridium(III) complexes **4** and **5**. These complexes exhibited only a similar or slightly better cytotoxic activity in comparison with the corresponding cationic ruthenium complexes of the type $[Ru(\eta^6\text{-}p\text{-cym})Cl\{Ph_2PCH_2CH_2CH_2SPh\text{-}\kappa P,\kappa S\}][PF_6]$ ($x=0$, 1).[37]

For further analysis, a thyroid carcinoma (8505C) cell line was selected as a model of a highly malignant and almost incurable type of tumor. 8505C cells were treated with the IC_{50} dose of complex **5** for 48 hours in order to explore the mechanism of action of iridium(III) complexes. Induction of apoptosis was analyzed with double Annexin V/propidium iodide (PI) staining. In comparison to the untreated control cells (early apoptosis 1.4%, late apoptosis/necrotic cells 5.7%), treatment with **5** for 48 hours gave rise to an increase in both early apoptotic cells (7.8%) marked by externalization of phosphatidylserin, stained by Annexin V, and late apoptotic/necrotic cells (36.5%), stained by both Annexin V and PI (Figure 3a). 8505C cells treated with complex **5** exhibited increased activation of caspases (**5**: 58.3%; control: 7.7%), indicating that caspase-dependent apoptosis is probably behind the action of this compound (Figure 3b). From the cell-cycle analysis, an increased percentage of hipodiploid cells with fragmented DNA upon treatment with **5** was observed (Figure 3c). The mechanism of cell death induced by complex **5** seems to be similar to the previously evaluated iridium(III) complex $[Ir(\eta^5\text{-}C_5Me_5)Cl_2\{Ph_2PCH_2S(O)Ph\text{-}\kappa P\}]$.[33] Thus, these results confirm that apoptosis is the dominant mode of action of this kind of iridium-based cytotoxic agents. While these compounds induce cell death through the same pathway, some differences in their biological effects could be observed. Complex **5** inhibits cell viability by 50% at a much lower concentration than $[Ir(\eta^5\text{-}C_5Me_5)Cl_2\{Ph_2PCH_2S(O)Ph\text{-}\kappa P\}]$, and it also induces significant apoptotic tumor cell death. In the cytoplasm of 8505C cells exposed to compound **5**, only a moderate enhancement of authophagic process was detected (**5**: 2.3%; control: 0.4%; Figure 3d). In contrast to $[Ir(\eta^5\text{-}C_5Me_5)Cl_2\{Ph_2PCH_2S(O)Ph\text{-}\kappa P\}]$, autophagy process is irrelevant for the effectiveness of complex **5**.

Previously, it was shown that $[Ir(\eta^5\text{-}C_5Me_5)Cl_2\{Ph_2PCH_2S(O)Ph\text{-}\kappa P\}]$ complex significantly decreased levels of free radicals—reactive oxygen species (ROS) and reactive nitrogen species (RNS)—in 8505C cells (24 h: 90%; 48 h: 95%).[33] In order to explore the involvement of oxidative stress in the cytotoxicity of **5**, cells were stained with the specific dye dihydrorhodamine 123 (DHR), which is sensitive to ROS and RNS. The cumulative effect was measured after 24 and 48 hours of exposure to complex **5**. The results obtained were in accordance with previously observed decreases in ROS/RNS levels in 8505C cells upon treatment with $[Ir(\eta^5\text{-}C_5Me_5)Cl_2\{Ph_2PCH_2S(O)Ph\text{-}\kappa P\}]$. Complex **5** decreased free radical levels in cells by more than 40% in comparison with control cells (Figure 4). From the literature, it is known that thyroid cancer cells treated with bortezomib, a proteasome inhibitor, demonstrated this phenomenon,

which was explained as a cell-specific response to toxic stimuli.[38,39] Namely, a decrease in the ROS level of thyroid cancer cells exposed to cytotoxic stimuli might occur as a result of elevated redox protection. Nevertheless, as in the case of $[Ir(\eta^5\text{-}C_5Me_5)Cl_2\{Ph_2PCH_2S(O)Ph\text{-}\kappa P\}]$ complex, this protection of the cells against oxidative stress did not have an influence on the effectiveness of complex **5**.

Conclusions

In the current study, neutral and cationic iridium(III) complexes of the type $[Ir(\eta^5\text{-}C_5Me_5)Cl_2\{Ph_2PCH_2CH_2CH_2S(O)_xPh\text{-}\kappa P\}]$ ($x=0$–2; **1**–**3**) and $[Ir(\eta^5\text{-}C_5Me_5)Cl\{Ph_2PCH_2CH_2CH_2S(O)_xPh\text{-}\kappa P,\kappa S\}][PF_6]$ ($x=0$–1; **4** and **5**) with 3-(diphenylphosphino)propyl phenyl sulfide, sulfoxide and sulfone ligands were synthesized, and their biological potential was proven against several cell lines. The following conclusions can be drawn (for an overview, see Figure 5):

1. The cytotoxic activities of examined iridium(III) complexes **1**, **2**, **4**, and **5** were found to be up to 25 times higher than that of cisplatin and up to 400 times higher than those of the corresponding ligands (**L1**–**L3**).
2. The different coordination mode (κP vs. $\kappa P,\kappa S$) of the $Ph_2PCH_2CH_2CH_2S(O)_xPh$ ligand ($x=0$, 1) does not significantly affect the cytotoxic activity of the iridium(III) complexes.
3. The oxidation state of sulfur in the ligands ($S(O)_2 < S(O) < S$) and the length of the spacer between the P and S atoms ($CH_2 < (CH_2)_3$) have a greater impact on the cytotoxic activities of the iridium(III) complexes in that the complexes with the $Ph_2PCH_2CH_2CH_2SPh$ and $PPh_2CH_2S(O)Ph$ ligands are the most active. Due to a possible oxidation of the pendant sulfur groups in vivo, the active species are unknown and the order of activities could vary in vivo.

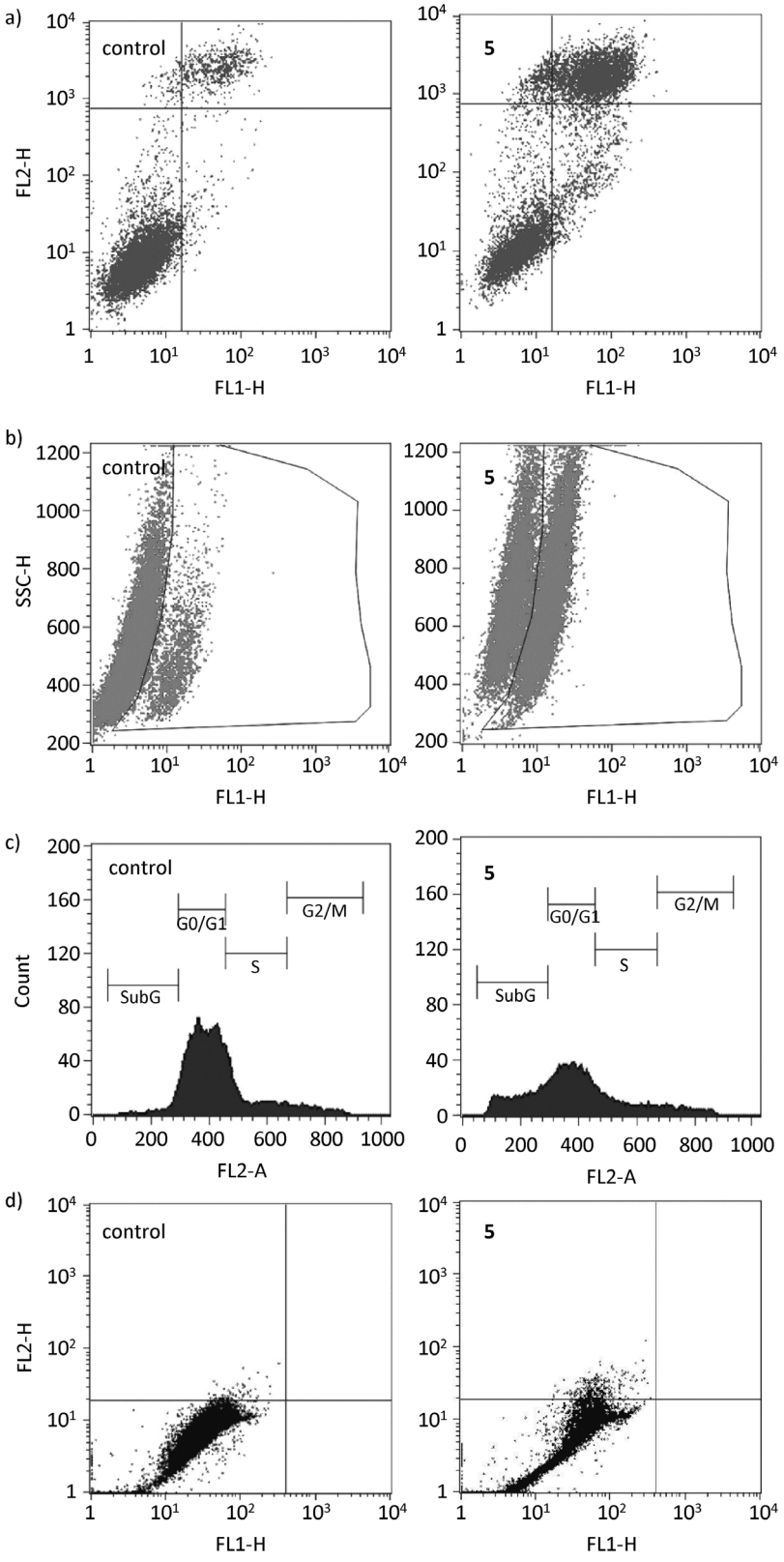

Figure 3. The effect of $[Ir(\eta^5\text{-}C_5Me_5)Cl\{Ph_2PCH_2CH_2CH_2S(O)Ph\text{-}\kappa P,\kappa S\}][PF_6]$ (**5**) on malignant cell death. 8505C cells were exposed to IC_{50} doses of compound **5**, and a) apoptosis, b) caspase activation, c) cell cycle distribution, d) presence of autophagic vesicles were investigated.

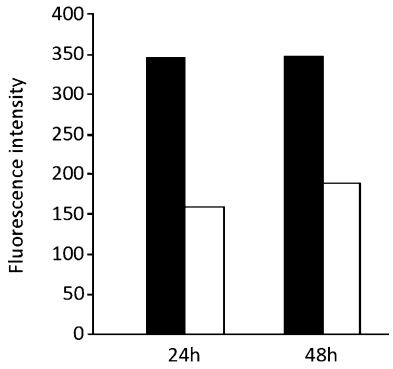

Figure 4. The effect of $[Ir(\eta^5\text{-}C_5Me_5)Cl\{Ph_2PCH_2CH_2CH_2S(O)Ph\text{-}\kappa P,\kappa S\}][PF_6]$ (**5**) on the levels of reactive oxygen (ROS) and nitrogen (RNS) species in 8505C cells: control (■) and complex **5** (□).

4. In all cell lines tested, neutral iridium(III) complexes **1**–**3** possess higher cytotoxic activities in comparison with the corresponding ruthenium(II) complexes $[Ru(\eta^6\text{-}p\text{-cym})Cl_2\{Ph_2PCH_2CH_2CH_2S(O)_x Ph\text{-}\kappa P\}]$ ($x = 0$, 1, 2).

In summary, for neutral and the cationic iridium(III) complexes **1**–**5**, a high biological potential, especially against highly aggressive, cisplatin-resistant tumor cell lines 8505C, MCF-7 and SW480, was observed. Importantly, apoptosis was shown to be the main pathway through which these complexes exert their cytotoxic action.

Experimental Section

Synthesis

General comments: All reactions and manipulations were carried out under argon using standard Schlenk techniques. Solvents were dried (*n*-pentane over Na/benzophenone; MeOH over magnesium; CH_2Cl_2 over CaH_2) and freshly distilled prior to use. NMR spectra (^1H, ^{13}C, ^{31}P) were recorded at 27 °C on Varian Gemini 200 and VXR 400 spectrometers. Chemical shifts (δ) are reported in parts per million (ppm) relative to residual solvent signals (CD_2Cl_2: $\delta_H = 5.32$ ppm, $\delta_C = 53.8$ ppm); δ_P values are relative to H_3PO_4 (85%) as an external reference. Microanalyses (C, H) were performed in the Microanalytical Laboratory of the Martin Luther University Halle-Wittenberg (Germany) using a CHNS-932 (LECO) elemental analyzer. $[\{IrCl_2(\eta^5\text{-}C_5Me_5)\}_2]$ and the ligands were prepared according to literature procedures.[40,41]

Preparation of $[IrCl_2(\eta^5\text{-}C_5Me_5)\{Ph_2PCH_2CH_2CH_2S(O)_x Ph\text{-}\kappa P\}]$ (1–3): A solution of $[\{IrCl_2(\eta^5\text{-}C_5Me_5)\}_2]$ (127 mg, 0.16 mmol) in CH_2Cl_2 (25 mL) was treated while stirring with the appropriate ligand (0.32 mmol), and the reaction was stirred at RT overnight. The resultant orange precipitate was isolated by filtration, washed with *n*-pentane (3×2 mL), and dried under vacuum to give the desired complexes as reddish powders.

Complex 1 ($x = 0$): Yield: 153 mg (65%); ^1H NMR (400 MHz, CD_2Cl_2): $\delta = 1.26$ (d, $^4J_{P,H} = 2.43$ Hz, 15H, CH_3), 1.29–1.34 (m, 1H, $CH_2CH_2CH_2$), 2.53–2.62 (m, 2H, $CH_2CH_2CH_2 + CH_2PPh_2$), 3.07–3.12 (m, 1H, SCH_2), 3.55–3.57 (m, 1H, CH_2PPh_2), 4.18–4.24 (m, 1H, SCH_2), 7.51–8.13 ppm (m, 15H, H_{Ph}); ^{13}C NMR (100 MHz, CD_2Cl_2): $\delta = 8.2$ (d, $^3J_{P,C} = 0.7$ Hz, CCH_3), 21.9 (s, $CH_2CH_2CH_2$), 25.1 (d, $^1J_{P,C} = 36.2$ Hz, CH_2PPh_2), 37.2 (s, SCH_2), 97.3 (d, $^2J_{P,C} = 2.1$ Hz, CCH_3), 123.7–135.5 ppm (C_{Ph}); ^{31}P NMR (162 MHz, CD_2Cl_2): $\delta = -2.4$ ppm (s); Anal. calcd for $C_{31}H_{36}Cl_2IrPS$ (MW = 734.78): C, 50.67; H, 4.94, found: C, 50.27; H, 4.76.

Complex 2 ($x = 1$): Yield: 178 mg (74%); ^1H NMR (400 MHz, CD_2Cl_2): $\delta = 1.33$ (d, $^4J_{P,H} = 2.16$ Hz, 15H, CH_3), 1.64–1.82 (m, 2H, $CH_2CH_2CH_2$), 2.59–2.78 (m, 2H, $SOCH_2$), 2.86–3.03 (m, 2H, CH_2PPh_2), 7.40–7.86 (m, 11H, H_{Ph}), 7.40–7.86 ppm (m, 4H, H_{Ph}); ^{13}C NMR (100 MHz, CD_2Cl_2): $\delta = 8.1$ (d, $^3J_{P,C} = 1.0$ Hz, CCH_3), 17.6 (s, $CH_2CH_2CH_2$), 26.0 (d, $^1J_{P,C} = 33.6$ Hz, CH_2PPh_2), 58.0 (s, $SOCH_2$), 92.1 (d, $^2J_{P,C} = 2.9$ Hz, CCH_3), 123.9–135.5 ppm (C_{Ph}); ^{31}P NMR (162 MHz, CD_2Cl_2): $\delta = -3.0$ ppm (s); Anal. calcd for $C_{31}H_{36}Cl_2IrOPS$ (MW = 750.78): C, 49.59; H, 4.83, found: C, 49.78; H, 5.01.

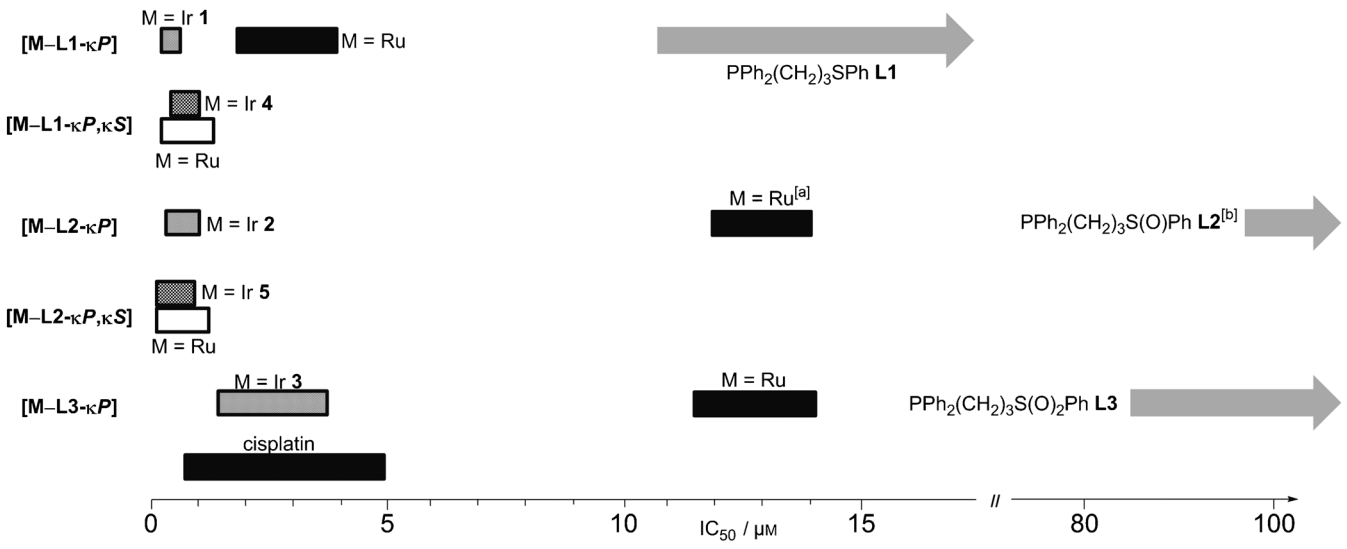

Figure 5. Range of cytotoxic activities, based on the IC_{50} values determined against the five cell lines under investigation, of iridium(III) complexes **1**–**5** ($[Ir] = Ir(\eta^5\text{-}C_5Me_5)Cl_x$; $x = 1$, 2) and of the related ruthenium(II) complexes $[Ru(\eta^6\text{-}p\text{-cym})Cl_2\{Ph_2PCH_2CH_2CH_2S(O)_x Ph\text{-}\kappa P\}]$ and $[Ru(\eta^6\text{-}p\text{-cym})Cl\{Ph_2PCH_2CH_2CH_2S(O)_x Ph\text{-}\kappa P,\kappa S\}][PF_6]$ ($[Ru] = Ru(\eta^6\text{-}p\text{-cym})Cl_x$; $x = 1$, 2). For comparison, the corresponding values of cisplatin and the uncoordinated ligands $Ph_2PCH_2CH_2CH_2S(O)_x Ph$ **L1**–**L3** are given. [a] Four values; exception: cell line MCF-7 ($IC_{50} = 1.8$ μM); [b] Four values; exception: cell line MCF-7 ($IC_{50} = 23.0$ μM).

Complex 3 ($x=2$): Yield: 174 mg (71%); ^{1}H NMR (400 MHz, CD_2Cl_2): $\delta=1.21$ (d, $^4J_{P,H}=2.19$ Hz, 15H, CH_3), 1.52–1.62 (m, 2H, $CH_2CH_2CH_2$), 2.74–2.80 (m, 2H, SO_2CH_2), 2.84–2.88 (m, 2H, CH_2PPh_2), 7.37–7.71 ppm (m, 15H, H_{Ph}); ^{13}C NMR (100 MHz, CD_2Cl_2): $\delta=8.7$ (d, $^3J_{P,C}=0.7$ Hz, CCH_3), 24.2 (s, $CH_2CH_2CH_2$), 37.2 (s, SO_2CH_2), 56.2 (d, $^1J_{P,C}=35.5$ Hz, CH_2PPh_2), 96.3 (d, $^2J_{P,C}=2.6$ Hz, CCH_3), 126.7–133.7 ppm (C_{Ph}); ^{31}P NMR (162 MHz, CD_2Cl_2): $\delta=-2.4$ ppm (s); Anal. calcd for $C_{31}H_{36}Cl_2IrO_2PS$ (MW=766.78): C, 48.56; H, 4.73, found: C, 48.21; H, 4.41.

Preparation of [IrCl(η^5-C_5Me_5){$Ph_2PCH_2CH_2CH_2S(O)_x$Ph-$\kappa P,\kappa S$}][PF_6] (4 and 5): A solution of [{$IrCl_2(\eta^5$-$C_5Me_5)$}$_2$] (127 mg, 0.16 mmol) in MeOH (30 mL) was treated while stirring with the appropriate ligand (0.32 mmol), and the reaction was heated at refux for 3 h. Next, [NH_4][PF_6] (6 equiv) was added, and the reaction mixture was stored at −70 °C overnight. The resultant precipitate was isolated by filtration, washed with Et_2O (3×2 mL), and dried under vacuum to give the desired complexes as yellow powders.

Complex 4 ($x=0$): Yield: 170 mg (63%); ^{1}H NMR (400 MHz, CD_2Cl_2): $\delta=1.22$ (d, $^4J_{P,H}=2.39$ Hz, 15H, CH_3), 1.30–1.38 (m, 1H, $CH_2CH_2CH_2$), 2.41–2.60 (m, 2H, $CH_2CH_2CH_2+CH_2PPh_2$), 2.99–3.03 (m, 1H, SCH_2), 3.51–3.60 (m, 1H, CH_2PPh_2), 4.20–4.26 (m, 1H, SCH_2), 7.52–8.09 ppm (m, 15H, H_{Ph}); ^{13}C NMR (100 MHz, CD_2Cl_2): $\delta=8.3$ (d, $^3J_{P,C}=0.7$ Hz, CCH_3), 22.3 (s, $CH_2CH_2CH_2$), 25.7 (d, $^1J_{P,C}=36.4$ Hz, CH_2PPh_2), 37.5 (s, SCH_2), 97.8 (d, $^2J_{P,C}=2.1$ Hz, CCH_3), 123.7–135.8 ppm (C_{Ph}); ^{31}P NMR (162 MHz, CD_2Cl_2): $\delta=-14.5$ (s), −144.6 ppm (sept, $^1J_{P,F}=710.4$ Hz, PF_6); Anal. calcd for $C_{31}H_{36}ClF_6IrP_2S$ (MW=844.29): C, 44.10; H, 4.30, found: C, 43.88; H, 4.13.

Complex 5 ($x=1$): Yield: 193 mg (70%); ^{1}H NMR (400 MHz, CD_2Cl_2): $\delta=1.26$ (d, $^4J_{P,H}=2.37$ Hz, 15H, CH_3), 2.00–2.14 (m, 1H, $CH_2CH_2CH_2$), 2.43–2.66 (m, 2H, $CH_2CH_2CH_2+CH_2PPh_2$), 3.28–3.32 (m, 1H, $SOCH_2$), 3.41–3.50 (m, 1H, CH_2PPh_2), 4.27–4.34 (m, 1H, $SOCH_2$), 7.54–8.14 ppm (m, 15H, H_{Ph}); ^{13}C NMR (100 MHz, CD_2Cl_2): $\delta=8.0$ (s, CCH_3), 17.2 (s, $CH_2CH_2CH_2$), 25.1 (d, $^1J_{P,C}=37.4$ Hz, CH_2PPh_2), 55.5 (s, $SOCH_2$), 100.7 (d, $^2J_{P,C}=1.5$ Hz, CCH_3), 123.7–135.6 ppm (C_{Ph}); ^{31}P NMR (162 MHz, CD_2Cl_2): $\delta=-14.1$ (s), −146.6 ppm (sept, $^1J_{P,F}=710.8$ Hz, PF_6); Anal. calcd for $C_{31}H_{36}ClF_6IrOP_2S$ (MW=860.29): C, 43.28; H, 4.22, found: C, 43.51; H, 4.42.

X-ray crystallography

Data for X-ray diffraction analyses of single crystals of complexes **3** and **4** were collected on an Oxford Gemini S diffractometer at 100 K using $Mo_{K\alpha}$ radiation ($\lambda=0.71073$ Å, graphite monochromator). A summary of the crystallographic data, the data collection parameters, and the refinement parameters are given in Table S3 of the Supporting Information. Multiscan absorption corrections were applied using SCALE3 ABSPACK (**3**: $T_{min}/T_{max}=0.69/1.00$; **4**: 0.55/1.00).[43,44] The structures were solved with direct methods using SHELXS-97 and refined using full-matrix least-square routines against F^2 with SHELXL-97.[45,46] All non-hydrogen atoms were refined with anisotropic displacement parameters, and hydrogen atoms with isotropic ones. Hydrogen atoms were placed in calculated positions according to the riding model. In complex **4**, the hydrogen atoms of the methyl groups were found to be disordered over two positions with occupancies of 50%. Furthermore, some restraints had to be used for the refinement of the Ir(η^5-C_5Me_5) fragment (DELU, SIMU, ISOR) in complex **4**. CCDC 972711 and 972712 contain the supplementary crystallographic data for this paper. These data can be obtained free of charge from The Cambridge Crystallographic Data Centre via www.ccdc.cam.ac.uk/data_request/cif.

In vitro assays

Reagents and cells: Fetal calf serum (FCS), RPMI-1640, phosphate-buffered saline (PBS), dimethyl sulfoxide (DMSO), and propidium iodide (PI) were obtained from Sigma (St. Louis, MO, USA). Annexin V-FITC (AnnV) was purchased from Biotium (Hayward, CA, USA). Acridin orange (AO) was obtained from Labo-Moderna (Paris, France). Apostat was purchased from R&D Systems (Minneapolis, MN, USA). Human thyroid carcinoma 8505C, submandibular gland carcinoma A253, breast adenocarcinoma MCF7, melanoma 518A2 and colon cancer SW480 were obtained from the ATCC. Cells are routinely maintained in 2-[4-(2-hydroxyethyl)piperazin-1-yl]ethanesulfonic acid (HEPES)-buffered RPMI-1640 medium supplemented with 10% FCS, 2 mM L-glutamine, 0.01% sodium pyruvate, and antibiotics (culture medium) at 37 °C in a humidified atmosphere with 5% CO_2. After standard trypsinization, cells were seeded at 1×10^3–2.5×10^3/well in 96-well plates for viability determination and 1.5×10^5/well in six-well plate for flow cytometry.

Determination of cell viability by sulforhodamine B assay (SRB): The viability of adherent viable cells was measured by an SRB assay.[35] Cells were exposed to a wide range of doses of test compound for 96 h and then fixed with 10% trichloroacetic acid (TCA) for 2 h at 4 °C. After fixation, cells were washed with distilled water, stained with 0.4% SRB solution for 30 min at RT, then washed and dried overnight. The dye was dissolved in 10 mM TRIS buffer, and the absorbance was measured at 540 nm with the reference wavelength at 640 nm. Results are expressed as percentage of control that was arbitrarily set to 100%.

Cell cycle analysis: Cells were treated with an IC_{50} dose of [Ir(η^5-C_5Me_5)Cl{$Ph_2PCH_2CH_2CH_2S(O)$Ph-$\kappa P,\kappa S$}][PF_6] (**5**) for 48 h, trypsinized, and fixed in 70% ethanol at 4 °C overnight. Cells were thoroughly washed in PBS, and stained with solution containing PI (20 μg mL^{-1}) and RNase (0.1 mg mL^{-1}) for 30 min at 37 °C in the dark. Red fluorescence was analyzed with a FACS Calibur flow cytometer (BD, Heidelberg, Germany). The distribution of cells in different cell-cycle phases was determined with Cell Quest Pro software (BD).[47]

AnnexinV-FITC/PI, AO staining and caspase detection: Cells were exposed to IC_{50} dose of [Ir(η^5-C_5Me_5)Cl{$Ph_2PCH_2CH_2CH_2S(O)$Ph-$\kappa P,\kappa S$}]-[PF_6] (**5**) for 48 h. After trypsinization, cells were stained with AnnV-FITC/PI (Biotium, Hayward, CA, USA) or Apostat according to the manufacturer's instruction. Alternatively, cells were stained with a solution of AO (100 μg mL^{-1}) for 15 min at 37 °C. Cells were analyzed with a FACS Calibur flow cytometer using Cell Quest Pro software.

Measurement of ROS generation: The production of reactive oxygen and nitrogen species was determined by redox-sensitive dye, dihydrorhodamine 123 (DHR). The cells were stained with 1 μM DHR for 20 min before treatment with [Ir(η^5-C_5Me_5)Cl{Ph_2PCH_2-$CH_2CH_2S(O)$Ph-$\kappa P,\kappa S$}][PF_6] (**5**). After 24 or 48 h incubation, cells were detached, washed with PBS, and the fluorescence intensity was analyzed with a FACS Calibur flow cytometer using Cell Quest Pro software.

Statistical analysis: Results are the mean ± standard deviation (SD) of triplicate observations from three experiments, unless indicated otherwise. The statistical significance between treatments and control was analyzed by ANOVA followed by a Student-Newman-Keul's test; $P<0.05$ was considered significant.

Acknowledgements

G.L. gratefully acknowledges financial support from the Graduiertenförderung des Landes Sachsen-Anhalt (Germany). The authors from the University of Belgrade (Serbia) would like to acknowledge financial support from the Ministry of Science and Technological Development of the Republic of Serbia (Grant No. 173013).

Keywords: apoptosis · cytotoxic agents · iridium(III) complexes · metal-based drugs · sulfur-functionalized phosphorus ligands

[1] *Bioorganometallics: Biomolecules, Labeling, Medicine*, (Ed.: G. Jaouen), Wiley-VCH, Weinheim, **2005**.
[2] B. Rosenberg, L. van Camp, T. Krigas, *Nature* **1965**, *205*, 698 – 699.
[3] B. Rosenberg, L. van Camp, J. E. Trosko, V. H. Mansour, *Nature* **1969**, *222*, 385 – 386.
[4] *Cisplatin: Chemistry and Biochemistry of a Leading Anticancer Drug*, (Ed.: B. Lippert), Wiley-VCH, Weinheim, **1999**.
[5] G. Chu, *J. Biol. Chem.* **1994**, *269*, 787 – 790.
[6] E. Wong, C. M. Giandomenico, *Chem. Rev.* **1999**, *99*, 2451 – 2466.
[7] M. Galanski, M. A. Jakupec, B. K. Keppler, *Curr. Med. Chem.* **2005**, *12*, 2075 – 2094.
[8] S. H. van Rijt, P. J. Sadler, *Drug Discovery Today* **2009**, *14*, 1089 – 1097.
[9] M. J. Clarke, F. Zhu, D. R. Frasca, *Chem. Rev.* **1999**, *99*, 2511 – 2534.
[10] Z. Guo, P. J. Sadler, *Angew. Chem.* **1999**, *111*, 1610 – 1630; *Angew. Chem. Int. Ed.* **1999**, *38*, 1512 – 1531.
[11] J. C. Dabrowiak, *Metals in Medicine*, Wiley, Chichester, **2009**.
[12] M. Cocchietto, G. Sava, *Pharmacol. Toxicol.* **2000**, *87*, 193 – 197.
[13] G. Sava, A. Bergamo, *Int. J. Oncol.* **2000**, *17*, 353 – 365.
[14] R. Gagliardi, G. Sava, S. Pacor, G. Mestroni, E. Alessio, *Clin. Exp. Metastasis* **1994**, *12*, 93 – 100.
[15] C. G. Hartinger, S. Zorbas-Seifried, M. A. Jakupec, B. Kynast, H. Zorbas, B. K. Keppler, *J. Inorg. Biochem.* **2006**, *100*, 891 – 904.
[16] J. M. Rademaker-Lakhai, D. van den Bongard, D. Pluim, J. H. Beijnen, J. H. M. Schellens, *Clin. Cancer Res.* **2004**, *10*, 3717 – 3727.
[17] M. A. Jakupec, V. B. Arion, S. Kapitza, E. Reisner, A. Eichinger, M. Pongratz, B. Marian, N. Graf von Keyserlingk, B. K. Keppler, *Int. J. Clin. Pharmacol. Ther.* **2005**, *43*, 595 – 596.
[18] G. Marcon, A. Casini, P. Mura, L. Messori, A. Bergamo, P. Orioli, *Metal-Based Drugs* **2000**, *7*, 195 – 200.
[19] S. J. Lucas, R. M. Lord, R. L. Wilson, R. M. Phillips, V. Sridharan, P. C. McGowan, *Dalton Trans.* **2012**, *41*, 13800 – 13802.
[20] K. K. W. Lo, K. Y. Zhang, *RSC Adv.* **2012**, *2*, 12069 – 12083.
[21] Y. Geldmacher, M. Oleszak, W. S. Sheldrick, *Inorg. Chim. Acta* **2012**, *393*, 84 – 102.
[22] H. Amouri, J. Moussa, A. K. Renfrew, P. J. Dyson, M. N. Rager, L.-M. Chamoreau, *Angew. Chem.* **2010**, *122*, 7692 – 7695; *Angew. Chem. Int. Ed.* **2010**, *49*, 7530 – 7533.
[23] S. Wirth, C. J. Rohbogner, M. Cieslak, J. Kazmierczak-Baranska, S. Donevski, B. Nawrot, I.-P. Lorenz, *J. Biol. Inorg. Chem.* **2010**, *15*, 429 – 440.
[24] A. Casini, F. Edafe, M. Erlandsson, L. Gonsalvi, A. Ciancetta, N. Re, A. Ienco, L. Messori, M. Peruzzini, P. J. Dyson, *Dalton Trans.* **2010**, *39*, 5556 – 5563.
[25] M. Gras, B. Therrien, G. Süss-Fink, A. Casini, F. Edafe, P. J. Dyson, *J. Organomet. Chem.* **2010**, *695*, 1119 – 1125.
[26] C. G. Hartinger, *Angew. Chem.* **2010**, *122*, 8482 – 8483; *Angew. Chem. Int. Ed.* **2010**, *49*, 8304 – 8305.
[27] L. Helm, A. E. Merbach, *Coord. Chem. Rev.* **1999**, *187*, 151 – 181.
[28] Y. Geldmacher, I. Kitanovic, H. Alborzinia, K. Bergerhoff, R. Rubbiani, P. Wefelmeier, A. Prokop, R. Gust, I. Ott, S. Wölfl, W. S. Sheldrick, *ChemMedChem* **2011**, *6*, 429 – 439.
[29] Z. Liu, A. Habtemariam, A. M. Pizarro, S. A. Fletcher, A. Kisova, O. Vrana, L. Salassa, P. C. A. Bruijnincx, G. J. Clarkson, V. Brabec, P. J. Sadler, *J. Med. Chem.* **2011**, *54*, 3011 – 3026.
[30] S. Schäfer, I. Ott, R. Gust, W. S. Sheldrick, *Eur. J. Inorg. Chem.* **2007**, 3034 – 3046.
[31] Z. Liu, L. Salassa, A. Habtemariam, A. M. Pizarro, G. J. Clarkson, P. J. Sadler, *Inorg. Chem.* **2011**, *50*, 5777 – 5783.
[32] Z. Liu, A. Habtemariam, A. M. Pizarro, G. J. Clarkson, P. J. Sadler, *Organometallics* **2011**, *30*, 4702 – 4710.
[33] G. Ludwig, S. Mijatović, I. Ranđelović, M. Bulatović, D. Miljković, D. Maksimović-Ivanić, M. Korb, H. Lang, D. Steinborn, G. N. Kaluđerović, *Eur. J. Med. Chem.* **2013**, *69*, 216 – 222.
[34] Cambridge Structural Database (ConQuest), Version 1.15, Crystallographic Data Centre, University Chemical Laboratory, Cambridge, UK, **2013**.
[35] P. Skehan, R. Storeng, D. Scudiero, A. Monks, J. McMahon, D. Vistica, J. T. Warren, H. Bokesch, S. Kenney, M. R. Boyd, *J. Natl. Cancer Inst.* **1990**, *82*, 1107 – 1112.
[36] G. Ludwig, G. N. Kaluđerović, M. Bette, M. Block, R. Paschke, D. Steinborn, *J. Inorg. Biochem.* **2012**, *113*, 77 – 82.
[37] G. Ludwig, G. N. Kaluđerović, T. Rüffer, M. Bette, M. Korb, M. Block, R. Paschke, H. Lang, D. Steinborn, *Dalton Trans.* **2013**, *42*, 3771 – 3774.
[38] Z.-X. Du, H.-Y. Zhang, X. Meng, Y. Guan, H.-Q. Wang, *BMC Cancer* **2009**, *9*, 56.
[39] Z.-X. Du, Y. Yan, H.-Y. Zhang, B.-Q. Liu, Y.-Y. Gao, X.-F. Niu, X. Meng, H-Q Wang, *J. Clin. Endocrinol. Metab.* **2011**, *96*, E763 – E771.
[40] R. G. Ball, W. A. G. Graham, D. M. Heinekey, J. K. Hoyano, A. D. McMaster, B. M. Mattson, S. T. Michel, *Inorg. Chem.* **1990**, *29*, 2023 – 2025.
[41] M. Block, M. Bette, C. Wagner, J. Schmidt, D. Steinborn, *J. Organomet. Chem.* **2011**, *696*, 1768 – 1781.
[42] M. Block, T. Kluge, M. Bette, J. Schmidt, D. Steinborn, *Organometallics* **2010**, *29*, 6749 – 6762.
[43] a) MULscanABS, PLATON for Windows Taskbar v1.15, University of Glasgow, **2008**; b) A. L. Spek, *J. Appl. Crystallogr.* **2003**, *36*, 7 – 13.
[44] SCALE3 ABSPACK, Empirical Absorption Correction, CrysAlis-Software package, Oxford Diffraction Ltd,**2006**.
[45] G. M. Sheldrick, SHELXS-97, Program for Crystal Structure Solution. University of Göttingen, Göttingen, **1998**.
[46] G. M. Sheldrick, SHELXL-97, Program for the Refinement of Crystal Structures. University of Göttingen, Göttingen, **1997**.
[47] G. N. Kaluđerović, S. Mijatović, B. B. Zmejkovski, M. Z. Bulatović, S. Gomez-Ruiz, M. Mojić, D. Steinborn, D. Miljković, H. Schmidt, S. D. Stošić-Grujičić, T. J. Sabo, D. Maksimović-Ivanić, *Metallomics* **2012**, *4*, 979 – 987.

Received: November 24, 2013
Published online on January 27, 2014